Real-Time Streaming Video With Adaptive Bandwidth Control and DCT-Based Error Concealment

Yon Jun Chung, JongWon Kim, and C.-C. Jay Kuo

***Abstract*— This work deals with dropped streaming video packets from the viewpoint of minimizing future dropped packets, as well as restoring data lost in packets already dropped, specifically geared toward real-time transmission of H.263+ bitstream. Minimization of future dropped packets is achieved by an adaptive least mean squares bandwidth (BW) controller predicting the available bandwidth supported by the Internet with relatively little loss. Restoration of lost video data is performed by a combination of error concealment (EC) techniques, including interpolation of border pixels in DCT domain. All algorithms presented are computationally inexpensive and thus suited for real-time video applications.**

***Index Terms*— Available bandwidth, feedback channel, least-mean-squares algorithm, real-time rate control, video streaming.**

I. Introduction

The Internet handles the real-time media transmission requirement by introducing a new protocol known as the real-time transport protocol (RTP) [1], which is built on top of the already-existing user datagram protocol (UDP). The characteristics of real-time video led to the selection of UDP over the reliable transmission control protocol (TCP). The reliability of TCP comes from its retransmission of dropped packets. However, it is not certain that retransmitted lost packets can arrive in a timely manner to be part of a playback already in progress. Thus, video applications that embraced TCP's reliability are forced to contend with either a large delay, or to postpone playback until all video data have been successfully received. Because packet loss is primarily a function of traffic, the performance of these products vary from being tolerable in light traffic to utter failure in heavy traffic.

The work presented in this paper is an effort to minimize the occurrence of packet loss through the use of a feedback channel, and mitigate packet loss through error concealment (EC). We propose a feedback-driven solution, where the sender and the receiver work in conjunction, adapting to the changing network condition to simultaneously minimize the number of dropped packets and conceal data contained in those missing packets. Real-time streaming protocol (RTSP) [2] is the protocol used in this work, since it employs the RTP/UDP setup, and conveniently comes with a ready-made control connection that can easily be extended to serve as a feedback channel.

What distinguishes the proposed feedback system from others is the miserly economy of bandwidth (BW) exercised with equal fervor on both packet loss minimization and EC fronts. We focus on one specific type of Internet video-streaming situation, where there is just one receiver for every sender. Thus, packet-loss minimization can be coordinated jointly between the sender and the receiver via the feedback channel. We further emphasize the delay-intolerant nature of real-time streaming video by inserting a modem connection in the data path [3]. Updates of changes in available BW and dropped packet frame locations are sparingly sent only as deemed necessary. That is, at the client's socket, network traffic vacillations including packet losses are detected. It is then exploited to help localize the dropped-packet effect and sustain the visual quality. In addition, by reducing BW as a response to packet loss, the transmitted RTP/UDP video exhibits network friendliness (i.e., using only a fair share amount of BW relative to the majority TCP) [4].

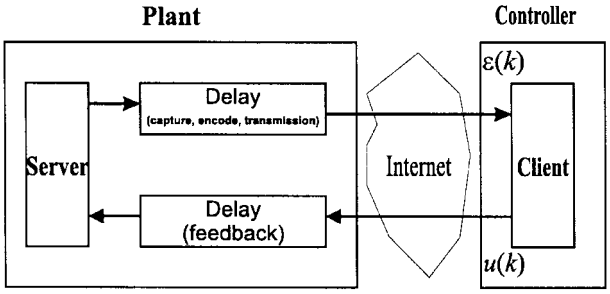

Fig. 1. The system block diagram for the adaptive LMS BW controller.

To control the propagation of visual artifacts due to packet loss, error-resilient encoding and error-concealment techniques should be applied in conjunction [5]. With the group of block (GOB) as the compromised packetization unit, the TCON model of H.263+ Test Model TMN-8 [6] is modified for motion-based EC. If the displacement vectors of missing macroblocks (MB's) are relatively small, motion-compensated replication can be effectively employed. While fast, the replication method can result in jagged and abrupt edge discontinuities with large motion content. A better spatial EC technique is needed in such cases, along with the intra-frame case. However, EC employing simple spatial interpolation often leads to blurred GOB of low resolution compared to their surrounding GOB's. An alternative EC based on the interpolation of DCT coefficients [7] is adopted here. It offers an improved resolution, yet has a complexity low enough to run in real time.

This paper is organized as follows. Section II describes an adaptive least mean squares (LMS) BW controller that coordinates the size of the transmitted video bitstream between the sender and the receiver. In Section III, we discuss a real-time DCT-based EC scheme. Experimental results for both packet-loss minimizing LMS-modulated bit streams and the computationally expedient EC counterparts are shown in Section IV. Finally, concluding remarks are given in Section V.

II. Adaptive LMS BW Controller

The LMS controller is a model-free controller developed in the context of statistical signal processing, as shown in Fig. 1. The adaptive LMS BW controller predicts currently available BW solely based on output observations $\epsilon(k)$. It treats the entire Internet as one massive Internet protocol (IP) cloud, with the sender and receiver as well-defined respective entry and exit points. The robust nature of LMS controllers make them applicable to nonlinear and nonstationary systems, such as the Internet. Observations include the sequence numbers, inter-arrival times, and timestamps of packets successfully

Manuscript received October 14, 1998; revised March 9, 1999. This work was supported by the Integrated Media Systems Center (a National Science Foundation Engineering Research Center) and by the Annenberg Center for Communication at the University of Southern California, Los Angeles, CA. This paper was recommended by Guest Editors F. Maloberti and M. Tummala.

Y. J. Chung and C.-C. J. Kuo are with the Integrated Media Systems Center and the Department of Electrical Engineering Systems, University of Southern California, Los Angeles, CA 90089-2564 USA.

J. W. Kim is with the Integrated Media Systems Center and the Department of Electrical Engineering Systems, University of Southern California, Los Angeles, CA 90089-2564 USA, and also with the Electronic Engineering Department, KongJu National University, KongJu, Korea.

Publisher Item Identifier S 1057-7130(99)05654-2.

arriving at the receiver's sockets. From the observation of $\epsilon(k)$, the receiver can infer the current traffic situation.

In return, the receiver can relay back any number of data to the sender including the packet-loss rate, the delay, and the available BW. Among these data, the available BW is the most useful parameter to a real-time rate controller. It can be used as a budget constraint in the rate-control calculation. We quantify the ratio of successfully arriving packet size over its transmission time as the currently sustainable bandwidth, and try to predict via the LMS controller the available bandwidth (ABW). The formulation for the LMS control can be described as [3]

$$\mathrm{ABW}_{k+1} = \mathrm{ABW}_k + 2\mu(\rho_{\mathrm{TH}} - \rho_k)\alpha_{\mathrm{pkt}}/\tau \tag{1}$$

where k denotes a time index according to some internal clock with a comparable resolution to the packet transmission clock, ρ_k is the packet-loss rate at time k, ρ_{TH} is threshold for the maximal acceptable packet-loss rate, α_{pkt} is the average size of the last few successfully transmitted packet, τ is the average inter-arrival time of the same set, and μ is the adaptation parameter determined through empirical tuning.

Since an overactive feedback channel may erode the data connection bandwidth, ABW updates are relayed to the sender only when a significant change in ABW is detected. For example, if there is a change in the packet-loss rate (i.e., the packet-loss rate ρ_k increases/decreases beyond the acceptable loss rate ρ_{TH}), the controller will enlarge/reduce the amount of the available bandwidth ABW_{k+1} of the next instance.

The rate controller at the sender (i.e., the encoder) must quickly respond to changes in updated ABW by adjusting the bitstream size correspondingly. However, the computational complexity and execution latency of the video encoder makes rate control in a microscale manner almost impossible. It is thus assumed that the short-term (instantaneous) fluctuation effect can be compensated by the smoothing effect of deployed encoder/decoder buffers. A longer time scale variation can be successfully modeled by considering time-varying constant bit rate (CBR) channels, where the available bandwidth is time varying and approximated with a piecewise-constant function. Here, we adopt a fast rate controller proposed in [8]. While most rate control algorithms examine bit allocation at the MB layer, this method handles the problem at the frame layer. Although technically challenging, it yields a greater degree of control over the spatio-temporal quality, resulting in a bitstream that satisfies the low latency requirement of CBR video better. This scheme allows us to estimate the optimal rate for the current frame according to a specific cost function (ABW, in this case) with low computational complexity and little added delay. Experimental results are given in Section IV-A to illustrate this point.

III. DCT-Based Error Concealment

If a large portion of a video frame is missing due to the loss of consecutive packets, EC methods are of very limited use. Our packet-loss minimizing-LMS effort described in Section II is implemented, essentially, to avoid multiple consecutive packet losses. Once the packet loss can be lowered to few consecutive packets, the EC response depends on the content of the lost packet.

Before any EC technique can be employed, the picture location corresponding to the data lost due to dropped packets must be determined. There are two synchronizing structures in H.263+: picture start code (PSC) and group of blocks start code (GBSC). They signal the start of a picture and a horizontal strip (GOB), respectively. For QCIF-sized sequences, each picture consists of nine GOB's, each of which consists of eleven 16×16 MB's. By comparing the last correctly transmitted GBSC with the next available

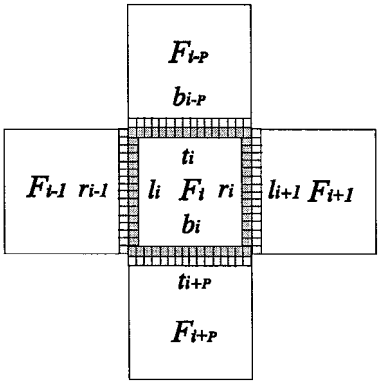

Fig. 2. Illustration of missing MB (F_i) with its four boundary vectors (t_i, b_i, l_i, and r_i) and their neighboring boundary vectors (b_{i-P}, t_{i+P}, r_{i-1}, and l_{i+1}) located inthe four adjacent MB (F_{i-P}, F_{i+P}, F_{i-1} and F_{i+1}), respectively.

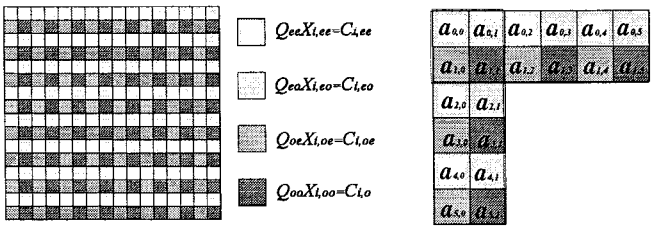

(a) (b)

Fig. 3. (a) DCT coefficient location of the four groups. (b) Selected 20 DCT coefficients in the implementation.

GBSC, the number of missing MB's can be inferred. Since the finest synchronization within one picture is the GBSC in H.263+, lost packets manifest themselves in missing horizontal strips.

Only the basic idea of the proposed spatial EC algorithm is presented here. We refer to [7] for more detail and mathematical derivation. Consider the missing MB represented by the center square F_i in Fig. 2. For QCIF image sequences, there are 9×11 MB's per picture $(P = 11)$, and each MB has 16×16 pixels, so that F_i is $N \times N$, with $N = 16$. It is reasonable to assume that boundary vectors $[t_i, b_i, l_i, r_i]$ of the missing MB are smoothly connected to their respective adjacent vectors, i.e., b_{i-P}, t_{i+P}, r_{i-1}, and l_{i+1}.

A suitable cost function can be expressed as

$$\psi = \|t_i - b_{i-P}\|^2 + \|b_i - t_{i+P}\|^2 + \|l_i - r_{i-1}\|^2 + \|r_i - l_{i+1}\|^2. \tag{2}$$

As mentioned earlier, lost packets in H.263+ result in missing horizontal strips. Thus, the horizontal adjacent vectors r_{i-1} and l_{i+1} are not available. They have to be first filled by linearly interpolating pixel pairs

$$\big(b_{i-(P+1)}(N-1), t_{i+P-1}(N-1)\big)$$

and

$$\big(b_{i-(P-1)}(0), t_{i+P+1}(0)\big)$$

respectively. By expressing the cost function in (2) in the frequency domain, and setting its first derivative to zero, we obtain the optimal solution X_i, which satisfies

$$\Psi'(X_i) = 0 \quad \text{and} \quad QX_i = C_i \tag{3}$$

where Ψ is the DCT of ψ, and Q is an $N^2 \times N^2$ matrix containing DCT kernel functions. After some manipulation, we can derive the

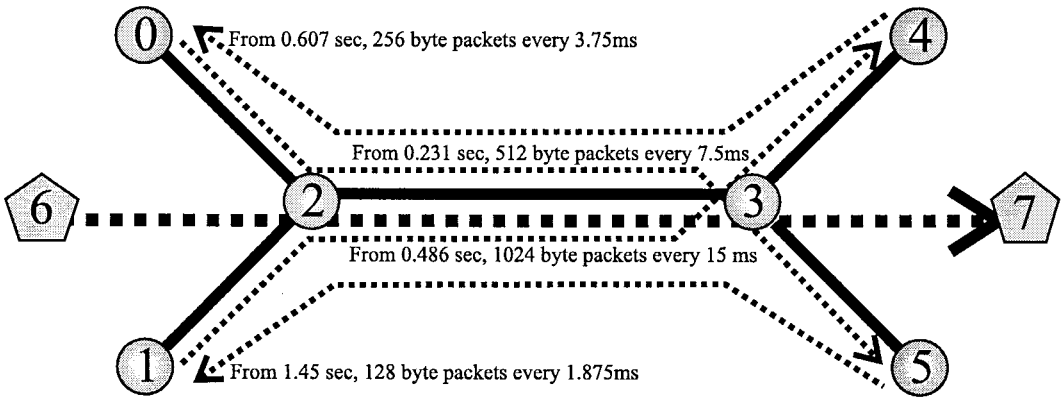

Fig. 4. Node configuration for the adaptive LMS controller simulation with NS, where thin dotted lines denote all other traffics except for the thick dotted traffic assigned for comparison.

following:

$$X_i = [a_{i,0,0} \cdots a_{i,0,N-1} a_{i,1,0} \cdots a_{i,1,N-1} a_{i,2,0} \cdots a_{i,N-1,N-1}]^T$$

and

$$C_i = \phi(0) \otimes \mathbf{b}_{i-P} + \phi(N-1) \otimes \mathbf{t}_{i+P} + \mathbf{r}_{i-1} \otimes \phi(0) + \mathbf{l}_{i+1} \otimes \phi(N-1)$$

where $\phi(n)$ are the DCT kernel functions and vectors $\mathbf{b}$, $\mathbf{t}$, $\mathbf{r}$, $\mathbf{l}$ are the DCT coefficient vectors of their spatial counterparts, $\otimes$ is the Kronecker-delta product. Simply speaking, $a_{i,n,m}$ are the two-dimensional (2-D) DCT coefficients of the missing MB F_i, while C_i is an $N^2 \times 1$ vector computed from DCT kernels and DCT of adjacent vectors. Equation (3) can be expanded as

$$\begin{aligned} QX_{i,n,m} &= 2\big(\phi_n^2(0) + \phi_m^2(0)\big) a_{i,n,m} \\ &\quad + \sum_{l=0, l\neq \frac{n}{2}}^{\frac{N}{2}-1} 2\phi_n(0)\phi_{2l}(0) a_{i,2l,m} \\ &\quad + \sum_{k=0, k\neq \frac{m}{2}}^{\frac{N}{2}-1} 2\phi_m(0)\phi_{2k}(0) a_{i,n,2k} \\ &= C_{i,n,m}. \end{aligned} \tag{4}$$

There are N^2 unknown 2-D DCT coefficients, while only $4N$ known border adjacent one-dimensional (1-D) DCT coefficients. This leads to a set of severely under-determined linear equations. To reduce the dimension of this set of equations, we can take advantage of the even and odd symmetries of DCT kernels, i.e.,

$$\phi_{\text{even}}(N-1) = \phi_{\text{even}}(0), \quad \phi_{\text{odd}}(N-1) = -\phi_{\text{odd}}(0). \tag{5}$$

By separating the set of equations in (3) into four groups according to even-odd pairings, i.e., Q_{ee}, Q_{eo}, Q_{oe}, and Q_{oo}, as shown in Fig. 3(a), we can exploit properties in (5) to down-select subsets of $N-1$ linearly independent equations within each group. In this manner, the reduced matrices Q_{xx} become invertible, so that $4(N-1)$ unknowns can be solved.

It is computationally expensive to solve for all $4(N-1)$ unknown DCT coefficients. As explained in [7], it is reasonable to solve 20 out of 60 for the case with $N = 16$. All other DCT coefficients are set to zero. In Fig. 3(b), we show the selected DCT coefficients in our implementation, where the index i has been dropped for brevity. The selection of $a_{n,m}$ is equivalent to choosing rows and columns of $\mathbf{A_i} = [a_{i,n,m}]$, the matrix to which IDCT must be performed to obtain the missing MB F_i. The fact that the inversion of four Q_{xx} matrices can be performed off-line is the main contribution to the computational simplicity of the above algorithm. A real-time version of the DCT-based EC algorithm has been implemented in our experiment as described in Section IV.

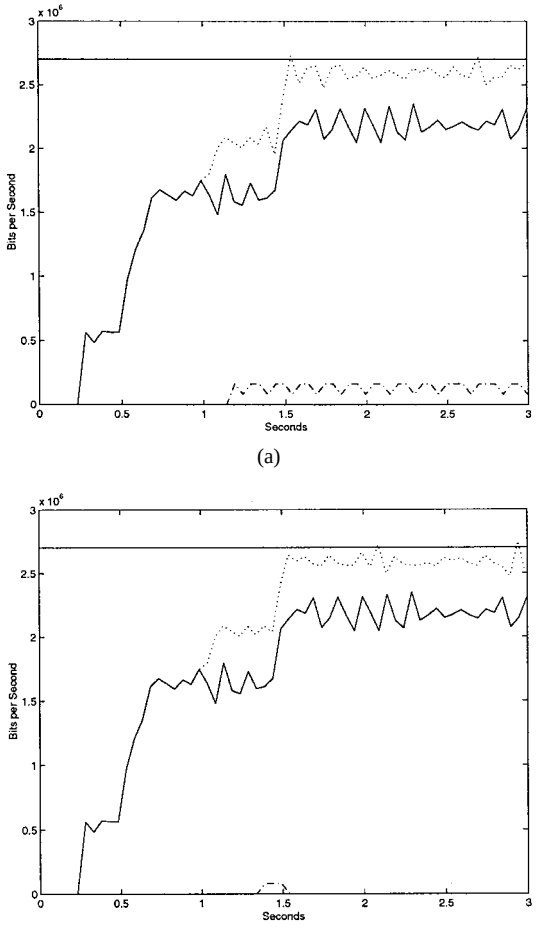

Fig. 5. Time traces of BW consumption (top traces) and loss (lower traces) on the bottleneck link from Node 2 to Node 3. (a) No BW control. (b) BW control, based on LMS BW feedback.

It is worthwhile to point out that the algorithm is specifically targeted for frames with very large motion vectors and intra-coded frames. In H.263+., an intra-coded frame usually occurs during a scene change, with no temporal correlation with its previous adjacent frame. In this scenario, the applicability of temporal EC methods is

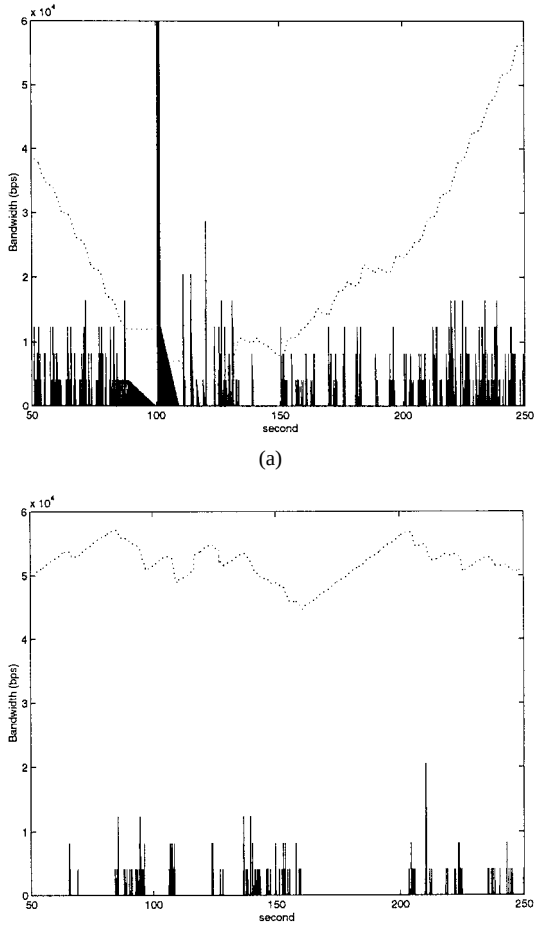

Fig. 6. Time trace of BW consumption, dotted line, and corresponding lost BW, solid line, due to dropped packets. (a) No rate control case. (b) LMS-controlled case.

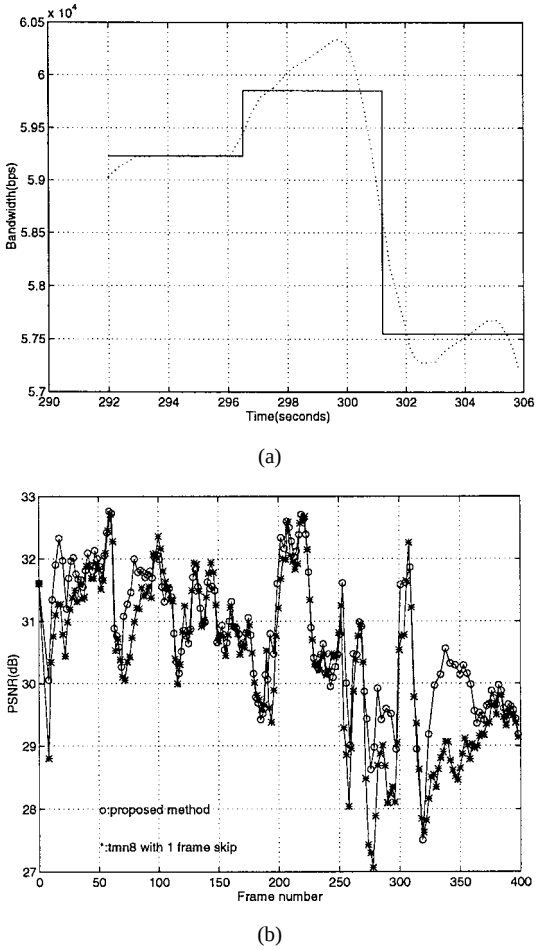

Fig. 7. (a) Dashed line is the ABW obtained using our LMS BW controller, and the solid line its piecewise approximation. (b) Using this BW approximation as our compression bit budget constraint, the PSNR comparison of our rate controller versus TMN-8.

limited. The fact that motion estimation in H.263+ is performed on adjacent pictures exacerbates the resolution deterioration. The adjacent picture dependency results in the propagation of reconstructed error pictures.

IV. Experimental Results

A. Adaptive Bandwidth Control

To measure the performance of the adaptive LMS BW controller, we conducted the following simulation using the NS software [9]. NS has been developed as a joint effort headed by Information Sciences Institute (ISI), a USC research laboratory, and Lawrence Berkeley National Lab (LBNL). Unlike experiments performed directly on the Internet, NS simulations result in a repeatable and consistent manner for easy performance comparisons. Due to the large scope of the Internet, NS simulations are rarely done using networks of a comparable size. Nevertheless, it is a capable tool to test network algorithms, and has been widely used among network researchers.

Let us consider a simple network configuration as shown in Fig. 4, where various streams are started at staggered times to result in traffic as shown in Fig. 5. The scheduled events are described in order as follows.

- Event 1: From $t = 0.231$, a bitstream of 512 byte packets are sent from Node 0 to Node 5 for every 7.5 ms.
- Event 2: From $t = 0.486$, a bitstream of 1024 byte packets are sent from Node 1 to Node 4 for every 15 ms.
- Event 3: From $t = 0.607$, a bitstream of 256 byte packets are sent from Node 4 to Node 1 for every 3.75 ms.
- Event 4: From $t = 1$, a test case bitstream is sent from Node 6 to Node 7.
- Event 5: From $t = 1.45$, a bitstream of 128 byte packets are sent from Node 5 to Node 1 for every 1.875 ms.

In this configuration, the main bottleneck link is from Node 2 to Node 3, whose maximum capacity is 2.7 Mbits/s, as indicated by the horizontal line given in Fig. 5. For Events 1–3 and 5, the average bit rates are the same, i.e., around 546 kbits/s. For Event 4, we test an adaptive LMS BW controlled bitstream and an bitstream without BW control or estimation starting from $t = 1$. The resulting packet loss on the bottleneck link is compared for these two cases. The objective of this experiment is to demonstrate that the LMS BW controlled bitstream should be able to reduce its BW consumption and consequently reduce packet loss in the face of heavier traffic at $t = 1.45$ while the uncontrolled bitstream cannot.

Let us examine Fig. 5 in greater detail. The sawtooth solid lines on Fig. 5(a) and (b) are identical. They are the result loading events 1, 2, 3, and 5, and plotted to indicate the test traffic pattern for our simulation. It is specifically shaped to trip up any non BW controlled stream starting prior to $t = 1.45$. At $t = 1.45$, the remaining capacity on the bottleneck link (i.e. the gap between the horizontal and the

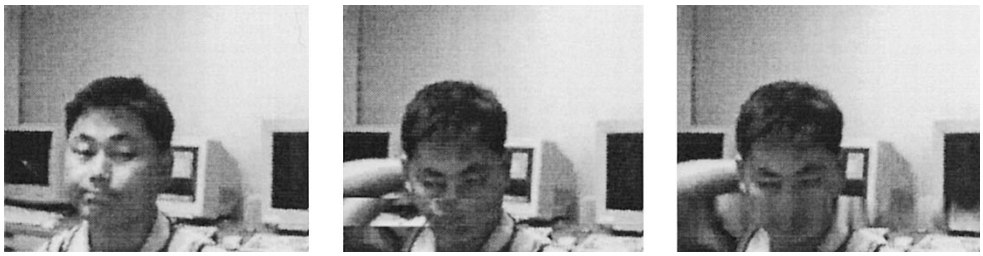

(a) (b) (c)

Fig. 8. Decompressed sequence with packet losses and different scenarios for EC selection. (a) An example where temporal EC is appropriate. (b) Temporal EC fails as motion content increases. (c) The restored image with the DCT-based EC under the same condition of (b).

sawtooth solid lines) begins to narrow. Therefore, any video stream starting before $t = 1.45$ must begin performing BW control, and essentially reduce its BW consumption according to perceived traffic. Otherwise, it will suffer major packet loss.

Fig. 5(a) shows the case without control. The upper dotted line represents the sum of the test traffic pattern and a video stream with no BW control while the lower dashed line represents the resulting packet loss. When this system continues to transmit at a constant rate even past 1.45 s, 5.1-Mbits worth of packets are lost for a video transmission duration of two seconds. The packet loss occurs after $t = 1.2$ and continues throughout the whole process. It is important to point out that dropped packets can also come from the other four streams sharing the Node 2 to Node 3 link. By contrast, our LMS BW controlled stream shown in Fig. 5(b) suffers fewer packet losses worth only 0.24-Mbits. It happens only for a short period time, around $t = 1.5$.

With a cursory glance, it may appear that the two dotted lines of Figs. 5(a) and (b) are the same. Upon closer inspection, they reveal themselves to be distinct yet similar. This result indicates that the proposed LMS BW controlled stream can achieve a BW consumption level very close to the none controlled case, yet suffer significantly fewer lost packets. Its implication is that the occurrence of clustered packet loss is reduced, hence making the presented EC algorithm effective. Furthermore, by consuming BW only attainable, the LMS BW controlled case diminishes its negative impact to other transmissions already in progress.

Experimental results performed on the real-world Internet environment (using the Internet modem connection as described in [3]) are shown in Fig. 6. Since this is the Internet environment, the execution of experiment with and without LMS BW control cannot be repeated under exactly identical traffic conditions. However, results shown in these plots are generally consistent with repeated attempts. On the average, noncontrolled bitstreams suffer a packet-loss rate of 23% in comparison with 4% for those using the LMS BW control. The most significant difference is the size of clustered packet losses.

The plots in Fig. 6(a) and (b) are the results of transmitting streaming video without BW control and with LMS BW control, respectively. The upper trace (the dotted line) in Fig. 6(a) and (b) denotes the BW consumption of successfully transmitted packets while the lower trace indicates the BW of dropped packets. In the beginning, encoders in both systems shown in Fig. 6(a) and (b) attempt to load the network with bitstream of the same size. When the end user in Fig. 6(a) fails to detect congestion and alter its bitstream, the system suffers increasing packet loss and culminates in the lost packet spike at $t = 101$. For this particular instance, the cluster packet loss is 144 packets within time span less than 1 s. By contrast, the largest clustered loss for the LMS controlled case is four packets. As shown in Fig. 6(b), the dropped packet mostly occurs in a single drop.

These Internet experiments elucidate again the self-feeding nature of congestion. The best policy for packet-loss minimization in the face of traffic is to reduce BW usage. The main questions are the amount of reduction and the execution manner. The proposed LMS BW controller turns out to be a simple yet effective choice.

It is worthwhile to compare the proposed BW controller with another popular controller known as the multiple decrease/single increase scheme. Let us pay attention to the BW usage level (i.e., the dotted line) in Fig. 6(a) at around $t = 110$. It is around 6 kbits/s. A rate-adaption scheme employing a tenfold decrease/single increase would have to shrink its bitstream size down to this level at the first sign of congestion (i.e., from 60 to 6 kbits/s). No such drastic action is taken with our LMS controller, while packet minimization is still achieved.

The added benefit of the smooth BW consumption transition of our LMS algorithm is that it is easier for a rate controlling encoder to follow. Consider a variable bit rate (VBR) channel with its available bandwidth given in the dotted line in Fig. 7(a) and its piecewise constant approximation. The adaptive LMS controller relays to the real-time rate controller at the server the available bandwidth, and the real-time frame rate controller employs the channel bandwidth approximation as a bitstream budget and performs the necessary rate adjustment. Under the same channel bandwidth, we compare the PSNR performance of our real-time frame rate controller with that obtained via TMN-8 in Fig. 7(b). Note that even though Fig. 7(a) and (b) are labeled with different scales horizontally [i.e., the second in (a) and the frame number in (b)], there is actually a one-to-one correspondence. That is, frame number 0 corresponds to $t = 290$, while frame number 400 corresponds to $t = 306$. We should pay special attention to $t = 301$ where the available BW drops around 3.8%. It is clear that the LMS BW control algorithm adapts to the bandwidth change and provides higher PSNR values for frames between 275 and 300 and between 320 and 360.

B. Error Concealment

Once the picture location corresponding to packet loss is determined by the GOB unit (i.e., missing horizontal strips) with the help of appropriately generated H.263+ packets, we can apply the proposed DCT-based EC in connection with the modified TCON method according to the type of data corruption. That is, in case of consecutive packet losses where the proposed spatial EC technique is not applicable, we should revert back to simple replication.

We examine a decompressed sequence with packet losses under different EC schemes as illustrated in Fig. 8(a)–(c). We show an example where temporal EC is sufficient in Fig. 8(a). As motion content increases, the temporal EC gradually fails, as seen in Fig. 8(b). Finally, the restored image by using the DCT-based EC under the same condition of Fig. 8(b) is given in Fig. 8(c) for comparison. The proposed algorithm can capture frequency characteristics such as edges since it interpolates from the DCT coefficient. This can be seen by comparing Fig. 8(b) and (c), with special attention to the

elbow and nose areas. The restored elbow and nose in Fig. 8(c) are located in the right regions, with their edges partially reconstructed. The proposed method strives to restore line orientation using the DCT information of border pixels, and gives a reasonable result (with slightly degraded quality).

Finally, it is important to note that, since EC technique can only serve as a temporary remedy to packet loss, a timely refresh of packet-loss remnants is highly desirable. For this purpose, we can easily tie our feedback channel with the error resilient Annexes of H.263+. H.263+ offers the choice in intra/inter coding on a MB basis. Based on error tracking through the feedback, the adaptive intra-refresh (AIR) technique can achieve the desired refreshing effect without too much network burden [5]. It uses only an incrementally larger amount of bits compared to a picture entirely inter-coded, and still has the desired result in removing the reconstruction error propagation. In addition to the AIR technique, another error resilience technique named reference picture selection (RPS) is also proposed in H.263+. This method is somewhat more complicated in comparison to AIR, but may be more effective in handling packet loss. It restricts and synchronizes the transition to the next reference (reference for motion prediction) frame only after the reconstruction of the same reference frame is completed without error at the client side. The bit usage of intra-coded MB's can be avoided at the cost of extra motion search. It is worthwhile to integrate AIR and RPS techniques into our current framework to achieve real-time video transmission with improved and more robust quality.

V. Conclusion

We examined the problem of real-time video streaming over the Internet. While previous efforts, including error concealment and rate control, have been presented as a solution to this problem, they only addressed it from one end of the server-client pair. A coordinated approach between the server and the client in dealing with lost packets and error from both network and end-user viewpoints was proposed in this work. An adaptive LMS BW controller was introduced to adjust the amount of video data uploaded to the network so that the packet loss can be minimized in face of network congestion. The adaptive LMS BW controller, which resides at the client end, sends a prediction of the available bandwidth to the server via a feedback signal that the network can sustain at a specified packet-loss rate. Simulation and actual Internet results are provided to demonstrate the superior performance of the proposed LMS bandwidth controller. The proposed DCT EC is a computationally expedient algorithm with acceptable performance that can well serve as a temporary precursor to the AIR/RPS integration.

References

[1] H. Schulzrinne, S. Casner, R. Frederick, and V. Jacobson, *RTP: A transport protocol for real-time applications*, Internet Draft, Internet Engineering Task Force, RFC 1889, Jan. 1996.

[2] H. Schulzrinne, A. Rao, and R. Lanphier, *Real time streaming protocol (RTSP)*, Internet Draft, Internet Engineering Task Force, RFC 2326, Feb. 1998.

[3] Y. Chung, J. Kim, and C.-C. J. Kuo, "Network friendly video streaming via adaptive LMS bandwidth control," presented at Int. Symp. Optical Science, Engineering, and Instrumentation, San Diego, CA, July 1998.

[4] S. Floyd and K. Fall, "Promoting the use of end-to-end congestion control in the Internet," *IEEE/ACM Trans. Networking*, to be published.

[5] N. Faber, B. Girod, and J. Villasenor, "Extensions of ITU-T recommendation H.324 for error-resilient video transmission," *IEEE Commun. Mag.*, pp. 120–128, June 1998.

[6] Standardization Sector, ITU Telecom. (1997). *Video coded test model near-term, Version 8 (TMN8)*, H.263 Ad-Hoc Group. [Online]. Available FTP: standard.pictel.com/video-site

[7] J. Park, J. Kim, and S. Lee, "DCT coefficient recovery based error concealment technique and application to the MPEG-2 bit stream error," *IEEE Trans. Circuits Syst. Video Technol.*, vol. 7, pp. 845–854, Dec. 1997.

[8] H. Song, J. Kim, and C.-C. J. Kuo, "Real-time motion-based H.263+ frame rate control," presented at SPIE Visual Communication and Image Processing '99, San Jose, CA.

[9] UCB/LBNL/VINT Network Simulator—NS (version2). [Online]. Available HTTP: http://www-mash.cs.berkeley.edu/ns/

A Systematic Technique for Designing Approximately Linear Phase Recursive Digital Filters

Kimmo Surma-aho and Tapio Saramäki

***Abstract*— A systematic method is introduced for designing approximately linear phase low-pass recursive digital filters. The filter structures under consideration are the conventional cascade-form realization and the parallel connection of two allpass filters (lattice wave digital filters). Given the amplitude specifications, the filter parameters as well as the slope of the linear phase response are optimized in such a way that the maximum phase deviation from this linear phase is minimized in the passband. The filters are designed such that either the maximum amplitude value in the transition band is less than or equal to the passband maximum or the amplitude response is monotonically decreasing in this band. The proposed design scheme consists of two basic steps. The first step involves finding, in a simpler manner, a good suboptimum filter. In the second step, this filter is then used as an initial filter for further optimization that is carried out by the second algorithm of Dutta and Vidyasagar. Several examples are included illustrating the efficiency of the proposed design scheme. They also show the superiority of the resulting recursive filters over their linear phase finite-impulse response equivalents, especially in narrow-band cases.**

***Index Terms*— All-pass filters, approximation, cascade-form realizations, lattice-wave digital filters, linear-phase recursive filters, optimization, parallel connections of two all-pass filters, recursive filters, phase approximations, simultaneous amplitude and phase approximations.**

I. Introduction

One of the most difficult problems in filter synthesis is the simultaneous optimization of the phase and amplitude responses of recursive digital filters. This is because the phase of recursive filters is inherently nonlinear and, therefore, the amplitude selectivity and phase linearity are conflicting requirements.

The most straightforward approach to arrive at a recursive filter having simultaneously a selective amplitude response and an approximately linear phase response in the passband region is to generate the filter in two steps. First, a filter with the desired amplitude response is designed. Then, the phase response of this filter is made approximately linear in the passband by cascading it with an allpass

Manuscript received October 18, 1998; revised March 9, 1999. This work was supported by the Academy of Finland. This paper was recommended by Guest Editors F. Maloberti, P. Diniz, and K. Jenkins.

K. Surma-aho is with Nokia (Schweiz) AG, CH-8005 Zürich, Switzerland.

T. Saramäki is with Signal Processing Laboratory, Tampere University of Technology, P.O. Box 557, FIN-33101, Tampere, Finland.

Publisher Item Identifier S 1057-7130(99)05657-8.